Inorg. Chem. **2008**, *47*, 4746−4751

Octahedral Tilting in $MM'X_4$ Metal-Oxide Organic Layer Structures

Marie Vougo-Zanda, Ekaterina V. Anokhina,† Selma Duhovic, Lumei Liu, Xiqu Wang, Oluwakemi A. Oloba, Thomas A. Albright, and Allan J. Jacobson*

Department of Chemistry, University of Houston, Houston, Texas 77204-5003

Received January 15, 2008

Three metal-oxide organic frameworks have been synthesized and characterized: vanadium 1,4-benzenedicarboxylate, $V_2O_2F_{0.6}(OH)_{1.4}(BDC)\cdot 0.4H_2O$ (**1**); indium 1,4-benzenedicarboxylate, $In_2F_{2.2}(OH)_{1.8}(BDC)\cdot 1.6H_2O$ (**2**); and aluminum 1,4-benzenedicarboxylate $Al_2F_3(OH)(BDC)$ (**3**). The three-dimensional structures of **1**, **2**, and **3** have the same framework topology as the previously reported vanadium (III) 1,4-benzenedicarboxylate, $V^{III}_2(OH)_2F_2(BDC)$. The frameworks consist of inorganic layers constructed from corner sharing ML_6 octahedra (M = V, In, Al and L = OH, F) linked by BDC ligands. The structures are related to a general class of perovskite-related layer structures with composition $MM'X_4$. The layers show characteristic distortions that can be related to tilting of the ML_6 octahedra. In particular the structure of **1** consists of O−V distances that strongly alternate along the *b* axis. The electronic consequences of this distortion then create a tilting of the 1,4-benzenedicarboxylate ligand about the *a* axis. Crystal data: **1**, orthorhombic, space group *Pmna*, $a = 7.101(2)$ Å, $b = 3.8416(11)$ Å, $c = 20.570(6)$ Å; **2**, orthorhombic, space group *Cmcm*, $a = 7.490(4)$ Å, $b = 21.803(1)$ Å, $c = 8.154(4)$ Å; **3**, monoclinic, space group $P2_1/m$, $a = 10.7569(8)$ Å, $b = 6.7615(3)$ Å, $c = 7.1291(3)$ Å, $\beta = 76.02(1)°$.

Introduction

In the last several years considerable attention has been given to a class of solids often referred to as coordination polymers or metal organic frameworks (MOFs).[1–14] These compounds represent an extension of classical coordination chemistry into systems that have extended connectivity. The extended connectivity can involve either organic or inorganic polymerization or both. [13] The majority of the initial work in this area has focused on design principles or crystal engineering and has led to increased understanding of the effects of secondary interactions such as hydrogen bonding and π-π interactions on extended structures[2,14] and to important concepts such as reticular synthesis.[8,9]

Metal-oxide organic frameworks (MOOFs) are a subset of the more general class of MOFs and are distinguished by the presence of extended metal-oxide layers[15] or metal-oxide chains[16] in their structures. The extended metal oxide $[-O-M-O-M-O-]^{\infty}_n$ component distinguishes this class of compounds from those with isolated metal centers[17] or small metal oxide clusters.[18] Even with this restricted definition, MOOFs are still a large class of microporous solids with diverse compositions and chemical properties such as absorption and catalytic activity.

* To whom correspondence should be addressed. E-mail: ajjacob@uh.edu. Telephone: (713) 743-2785. Fax: (713) 743-2787.

† Deceased.

(1) Cheetham, A. K.; Férey, G.; Loiseau, T. *Angew. Chem., Int. Ed.* **1999**, *38*, 3268–3292.
(2) Moulton, B.; Zaworotko, M. J. *Chem. Rev.* **2001**, *101*, 1629–1658.
(3) Kesanli, B.; Lin, W. *Coord. Chem. Rev.* **2003**, *246*, 305–326.
(4) Rosseinsky, M. J. *Microporous Mesoporous Mater.* **2004**, *73*, 15–30.
(5) Rosi, N. L.; Eddaoudi, M.; Kim, J.; O'Keeffe, M.; Yaghi, O. M. *CrystEngComm* **2002**, *4*, 401–404.
(6) Férey, G. *Chem. Mater.* **2001**, *13*, 3084–3098.
(7) James, S. L. *Chem. Soc. Rev.* **2003**, *32*, 276–288.
(8) O'Keeffe, M.; Eddaoudi, M.; Li, H.; Reineke, T.; Yaghi, O. M. *J. Solid State Chem.* **2000**, *152*, 3–20.
(9) Yaghi, O. M.; O'Keeffe, M.; Ockwig, N. W.; Chae, H. K.; Eddadoudi, M.; Kim, J. *Nature* **2003**, *423*, 705–714.
(10) Yaghi, O. M.; Li, G.; Li, H. *Nature* **1995**, *378*, 703–706.
(11) Chae, H. K.; Siberio-Perez, D. Y.; Kim, J.; Go, Y.; Eddaoudi, M.; Matzger, A. J.; O'Keeffe, M.; Yaghi, O. M. *Nature* **2004**, *427*, 523–527.
(12) Kitagawa, S.; Kitaura, R.; Noro, S. *Angew. Chem., Int. Ed.* **2004**, *43*, 2334–2375.
(13) Cheetham, A. K.; Rao, C. N. R.; Feller, R. K. *Chem. Commun.* **2006**, 4780–4795.
(14) Lu, J.; Yu, C.; Niu, T.; Paliwala, T.; Crisci, G.; Somosa, F.; Jacobson, A. J. *Inorg. Chem.* **1998**, *37*, 4637–4640.
(15) (a) Johnson, J. W.; Jacobson, A. J.; Rich, S. M.; Brody, J. F. *J. Am. Chem. Soc.* **1981**, *103*, 5246–5247. (b) Johnson, J. W.; Jacobson, A. J.; Rich, S. M.; Brody, J. F. *Rev. Chim. Miner.* **1982**, *19*, 420–431.
(16) Zheng, L.-M.; Whitfield, T.; Wang, X.; Jacobson, A. J. *Angew. Chem., Int. Ed.* **2000**, *39*, 4528–4531.
(17) Lu, J.; Paliwala, T.; Lim, S. C.; Yu, C.; Niu, T.; Jacobson, A. J. *Inorg. Chem.* **1997**, *36*, 923–929.
(18) Li, H.; Eddaoudi, M.; O'Keeffe, M.; Yaghi, O. M. *Nature* **1999**, *402*, 276–279.

10.1021/ic8000448 CCC: $40.75
Published on Web 04/29/2008

Relative to the microporous coordination polymers with isolated metal centers, they typically have enhanced thermal stability that in some cases approaches that of zeolites and aluminophosphates.[19]

Several examples of metal oxide organic frameworks containing metal-oxide chains connected by coordinated metal ions[19,20] and layers or chains connected by bridging organic ligands, particularly 1,4-benzene dicarboxylate (BDC), have been reported. The MOHBDC [M = V(III), V(IV), Cr(III), and Al(III)] compounds first synthesized by Férey[21–26] and with [M = In(III), Fe(III), Fe(II), Al(III), Ga(III) and Y(III)] by us are examples of metal-oxide chains in this class of structures.[27–30] One related compound, $V^{III}_2(OH)_2F_2(BDC)\cdot H_2O$, MIL-71, which contains corner-shared MX_4 (X =F, OH) layers rather than chains connected by BDC ligands has been reported.[31] The layer structure is preserved on oxidation of V(III) to V(IV) in a polycrystalline sample, but the quality of the powder X-ray data was insufficient to refine the structure. In the present work, we report the synthesis and single crystal structure determination of the V(IV) compound $V_2O_2F_{0.6}(OH)_{1.4}(BDC)\cdot 0.4H_2O$ (**1**) and the analogous indium compound $In_2F_{2.2}(OH)_{1.8}(BDC)\cdot 1.6H_2O$ (**2**). The synthesis of $Al_2F_{3.3}(OH)_{0.7}(BDC)$ (**3**) and its structure determined from powder X-ray diffraction (XRD) are also described. The differences in the distortions of the ideal octahedral layers in the V(III), V(IV), In(III), and Al(III) compounds are discussed in terms of cooperative octahedral tilting.

Experimental Section

Synthesis. All chemicals purchased were of reagent grade and used without further purification. For **2** and **3**, Teflon bags were used to control the diffusion of water into the reactants, a technique which we have found to improve product crystallinity.

$[V_2O_2F_{0.6}(OH)_{1.4}(BDC)\cdot 0.4H_2O]$(1). Compound **1** was synthesized from a mixture of vanadium dioxide (3.5 mmol), 1,4-benzene dicarboxylic acid (1.74 mmol), HF (48%, 2.8 mmol), HCl (0.6 mmol), and deionized water (2.56 mL) in the molar ratios of 1:0.5:0.8:0.2:140. The starting chemicals and deionized water were mixed in a hydrothermal reaction vessel and heated at 220 °C for 4 d. After quenching to room temperature, the product was filtered and washed with dimethylsulfoxide (DMSO) to dissolve unreacted H_2BDC. The product was then dried at room temperature. The final product was a single phase containing single crystals of **1** in the form of blue-purple plates. The final pH of the reaction was approximately ~1–2.

$[In_2F_{2.2}(OH)_{1.8}(BDC)\cdot 1.6H_2O]$ (2). Compound **2** was synthesized from a mixture of indium (1 mmol), 1,4-benzenedicarboxylic acid (1 mmol), HF (48%, Merck, 0.02 mL), and deionized water (5 mL) in the molar ratios of 1:1:0.5:280. The starting chemicals including HF were mixed in a flexible Teflon bag (3 × 15 cm) in air. The bag was then placed in a hydrothermal reaction vessel containing 5 mL of deionized water and heated at 220 °C for 3 d. After quenching to room temperature, the product was filtered and washed with DMSO to dissolve unreacted H_2BDC. The product was then dried at room temperature. The final product was a single phase containing colorless single crystals of **2**. The final pH was approximately ~1–2.

$[Al_2F_{3.3}(OH)_{0.7}(BDC)]$ (3). Compound 3 was synthesized from a mixture of aluminum nitrate (1 mmol), 1,4-benzenedicarboxylic acid (1 mmol), HF (48%, Merck, 0.02 mL), and deionized water (10 mL) in the molar ratios of 1:1:0.5:560. The starting chemicals including HF were mixed in a flexible Teflon bag (3 × 15 cm) in air. The bag was then placed in a hydrothermal reaction vessel containing 10 mL of deionized water and heated at 220 °C for 3 d. After quenching to room temperature, the product was filtered and washed with DMSO to dissolve unreacted H_2BDC. The product was then dried at room temperature. The final product was a colorless polycrystalline phase of $Al_2F_{3.3}(OH)_{0.7}(BDC)$. The final pH was approximately ~1–2.

Elemental Analyses. Elemental analyses were performed by Gailbraith Laboratories (Knoxville, TN). Compounds **1**, **2**, and **3** were first formulated through crystal structure determination and chemical analysis results and then confirmed by thermogravimetric analysis. The observed and calculated chemical compositions are as follows $V_2O_2F_{0.6}(OH)_{1.4}(BDC)\cdot 0.4H_2O$ (**1**): V, 30.60% obs. (29.77% calc.); C, 27.45% obs. (28.05% calc.); H, 1.93% obs. (1.81% calc.); F, 3.49% obs. (3.33% calc.); $In_2F_{2.4}(OH)_{1.6}(BDC)\cdot 2.6H_2O$ (**2**): In, 43.90% obs. (46.41% calc.); C, 18.87% obs. (19.40% calc.); H, 2.08% obs. (1.82% calc.); F, 8.57% obs. (8.45% calc.); $Al_2F_{3.3}(OH)_{0.7}$ (BDC) (**3**): Al, 18.70% obs. (18.48% calc.); C, 32.08% obs. (32.91% calc.); H, 1.70% obs. (1.62% calc.); F, 21.67% obs. (21.47% calc.).

Computational Details. All calculations were carried out at the ab initio level with the B3LYP hybrid functional within the GAUSSIAN 03 program.[32] The basis sets for C and H were at the 3–21G level while that used for O was 6–31+G. The LANL2DZ pseudopotentials and associated basis was used for vanadium.

Characterization. The thermal decomposition behavior of compounds **1**, **2**, and **3** was determined by heating them in air at 3 °C/min on a TA instruments thermogravimetric analyzer. X-ray powders of the residues indicate the presence of $VO_{2.5}$, $InO_{1.5}$, and $AlO_{1.5}$ for compound **1**, **2**, and **3** respectively. However, the thermogravimetric data are not consistent with complete conversion to oxide phases. Because all three compounds contain fluoride, it is assumed that some fluoride remains in the TGA residues even though the specific phases cannot be detected by XRD. The TGA data indicate final compositions corresponding to 90% $VO_{2.5}$ and 10% VOF_3 for compound **1**, 60% $InO_{1.5}$ and 40% InF_3 for compound **2**, and an equal amount of $AlO_{1.5}$ and AlOF for compound **3**.

(19) Huang, J. *Ph. D. Thesis, University of Houston*, 2004.
(20) Do, J.; Jacobson, A. J. *Inorg. Chem.* **2001**, *40*, 2468–2469.
(21) Millange, F.; Serre, C.; Férey, G. *Chem. Commun.* **2002**, 822–823.
(22) Barthelet, K.; Marrot, J.; Riou, D.; Férey, G. *Angew. Chem., Int. Ed.* **2002**, *41*, 281–284.
(23) Serre, C.; Millange, F.; Thouvenot, C.; Nogues, M.; Marsolier, G.; Louer, D.; Férey, G. *J. Am. Chem. Soc.* **2002**, *124*, 13519–13526.
(24) Barthelet, K.; Marrot, J.; Férey, G.; Riou, D. *Chem. Commun.* **2004**, 520–521.
(25) Férey, G.; Latroche, M.; Serre, C.; Millange, F.; Loiseau, T.; Percheron-Guegan, A. *Chem. Commun.* **2003**, 2976–2977.
(26) Loiseau, T.; Serre, C.; Huguenard, C.; Fink, G.; Taulelle, F.; Henry, M.; Bataille, T.; Férey, G. *Chem.—Eur. J.* **2004**, *10*, 1373–1382.
(27) Whitfield, T. R.; Wang, X.; Liu, L.; Jacobson, A. J. *Solid State Sci.* **2005**, *7*, 1096–1103.
(28) Anokhina, E. V.; Vougo-Zanda, M.; Wang, X.; Jacobson, A. J. *J. Am. Chem. Soc.* **2005**, *127*, 15000–15001.
(29) Vougo-Zanda, M.; Wang, X.; Jacobson, A. J. Influence of Ligand Geometry on the Formation of In-O Chains in MOOFs (Metal-Oxide Organic Frameworks), to be published.
(30) Vougo-Zanda, M.; Wang, X.; Jacobson, A. J., unpublished results.
(31) Barthelet, K.; Adil, K.; Millange, F.; Serre, C.; Riou, D.; Ferey, G. *J. Mater. Chem.* **2003**, *13*, 2208–2212.
(32) Frisch, M. J. et. al. *Gaussian 03*, Revision B.03; Gaussian Inc.: Pittsburgh, PA, 2003; the full citation is given in the Supporting Information.

Table 1. Crystallographic Data for Compounds **1** and **2**

	1	**2**
chemical formula	$V_2O_2F_{0.6}(OH)_{1.4}(BDC)\cdot 0.4H_2O$	$In_2F_{2.2}(OH)_{1.8}(BDC)\cdot 1.6H_2O$
fw	346.8	494.8
cryst syst	orthorhombic	orthorhombic
space group	*Pmna*	*Cmcm*
a, Å	7.101(2)	7.490(4)
b, Å	3.8416(11)	21.803(11)
c, Å	20.570(6)	8.154(4)
V, Å^3	561.2(3)	1331.6(11)
Z	2	4
temp, K	293(2)	293(2)
ρ_c, g cm^{-3}	2.018	2.411
μ(Mo Kα), mm^{-1}	1.701	3.504
R1, wR2 [$I > 2\sigma(I)$][a]	0.0290, 0.0909	0.0658, 0.1046
R1, wR2 (all data)[a]	0.0298, 0.0912	0.1009, 0.1157

[a] $R1 = \sum||F_o| - |F_c||/\sum|F_o|$. $wR2 = [\sum w(F_o^2 - F_c^2)_2/\sum w(F_o^2)^2]^{1/2}$

The IR spectra were recorded on a Galaxy FTIR (Fourier Transform Infrared) 5000 series spectrometer at room temperature in the range of 4000–400 cm^{-1} using the KBr pellet method.

X-ray single crystal analyses for **1** and **2** were performed using a Siemens SMART platform diffractometer outfitted with a 1K CCD area detector and monochromatized graphite Mo Kα radiation. The structures were solved by direct methods and refined using SHELXTL. Crystal data for compounds **1** and **2** are summarized in Table 1.

The structure of $Al_2F_{3.3}(OH)_{0.7}(BDC)$ (**3**) was determined from powder XRD data and Rietveld analysis.[33] The powder XRD patterns were collected at room temperature on a Scintag XDS 2000 (Bragg–Brentano geometry, θ-θ mode) laboratory diffractometer with λ(Cu Kα1, Kα2) = 1.540562, 1.544390 Å.

Preliminary fast scan diffraction patterns of $Al_2F_{3.3}(OH)_{0.7}(BDC)$ showed very strong sharp peaks but with pronounced preferred orientation. To minimize this problem, a sample was sieved (using a 60-mesh sieve) onto a rectangular glass plate. The sieved powder was then slightly pressed down with a rough surface to further reduce orientation effects. The final X-ray pattern was taken from 7 to 70° with 2° divergence and 4° scattering slits, in the steps of 0.02° with 17 s counting time per step.

The powder pattern of $Al_2F_{3.3}(OH)_{0.7}(BDC)$ suggested that the compound has a layered structure. Indexing the pattern gave lattice parameters similar to those of compound **2** which were determined from single crystal X-ray data. Therefore, the atomic positions from this compound were used as a preliminary starting model.

The structure was refined using the GSAS-EXPGUI software package.[34] A set of background points were manually selected, fit to a polynomial function and then refined. The profile was refined using a modified Pseudo-Voigt profile function. The unit cell and the zero point error were also refined. It became apparent at this stage that the structure was monoclinic with space group $P2_1/m$, a subgroup of *Cmcm*. The lattice parameters are given in Table 2. The structure was refined by the Rietveld method with the atomic coordinates of $In_2F_{2.2}(OH)_{1.8}(BDC)\cdot 1.6H_2O$ as the starting model. Soft constraints on (Al−O and C−O) bond distances were applied, and the atomic coordinates of the aluminum and oxygen atoms refined. The carbon and oxygen atom positions were then refined separately. The bond constraints were removed, and a constraint added to the BDC anion. All the atomic coordinates at this point were refined simultaneously. The thermal parameters were constrained to be equal for each atom type, initially set to 0.025 and then refined.

(33) Rietveld, H. *J. Appl. Crystallogr.* **1969**, *2*, 65.
(34) Larson, A. C.; Von Dreele, R. B. *General Structure Analysis System (GSAS)*; Report LAUR 86–748; Los Alamos National Laboratory: Los Alamos, NM, 2000.

Table 2. Crystallographic Data and Structure Refinement Parameters for Compounds **3**

chemical formula	$Al_2F_{3.3}(OH)_{0.7}(C_8H_4O_4)$
formula weight (g/mol)	292.09
crystal system	monoclinic
space group	$P2_1/m$
a (Å)	10.7569(8)
b (Å)	6.7615(3)
c (Å)	7.1291(3)
β (°)	76.02(1)
V (Å^3), Z	503.17(6), 2
T (K)	298
λ(Cu Kα), Kα_2/Kα_1	1.54050, 1.54430; 0.5
2θ range (°)	7–70
no. reflections	506
no. independent atoms	13
no. structural parameters	26
no. profile parameters	9
no. soft constraints	16
overall R_P	0.0962
overall R_{WP}	0.1374
$R_{Bragg}(F^2)$	0.1833
converged χ^2	0.4515
background function	Chebyshev 1st kind
profile function	Pseudo-Voigt

The formula deduced from the structure determination is $Al_2L_4(BDC)$ where L = F or/and OH. The final formula deduced from the chemical analysis is $Al_2F_{3.3}(OH)_{0.7}(BDC)$. A summary of the results of the structure refinements is given in Table 2. The final Rietveld plots are shown in Figure 1.

Results and Discussion

The structures of all three compounds (Figure 2) consist of inorganic layers constructed from corner sharing ML_6 (M = In, V, Al and L = O and/or F) octahedra linked by BDC ligands (BDC= 1,4-benzenedicarboxylate). The structure of $V_2O_2F_{0.6}(OH)_{1.4}(BDC)\cdot 0.4H_2O$ (**1**) is shown in Figure 1a. The compound contains V(IV), and like other high oxidation state vanadium oxides, the $VO_{4/2}(L)_{2/2}$ octahedra are distorted

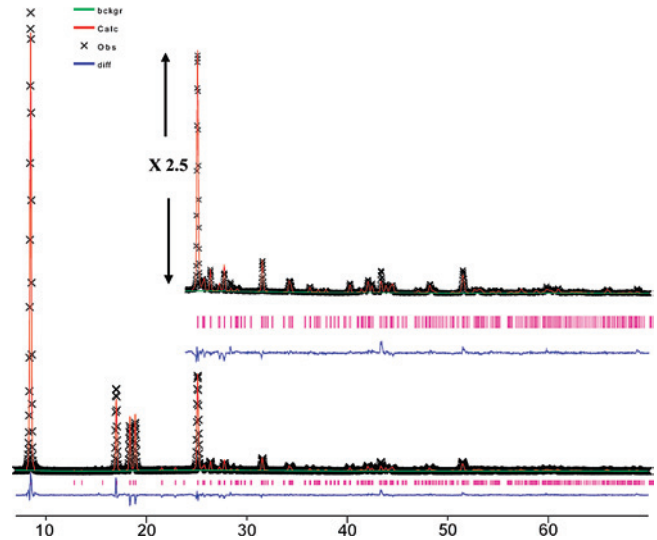

Figure 1. Final Refined Powder X-ray Data for $Al_2F_{3.3}(OH)_{0.7}(BDC)$.

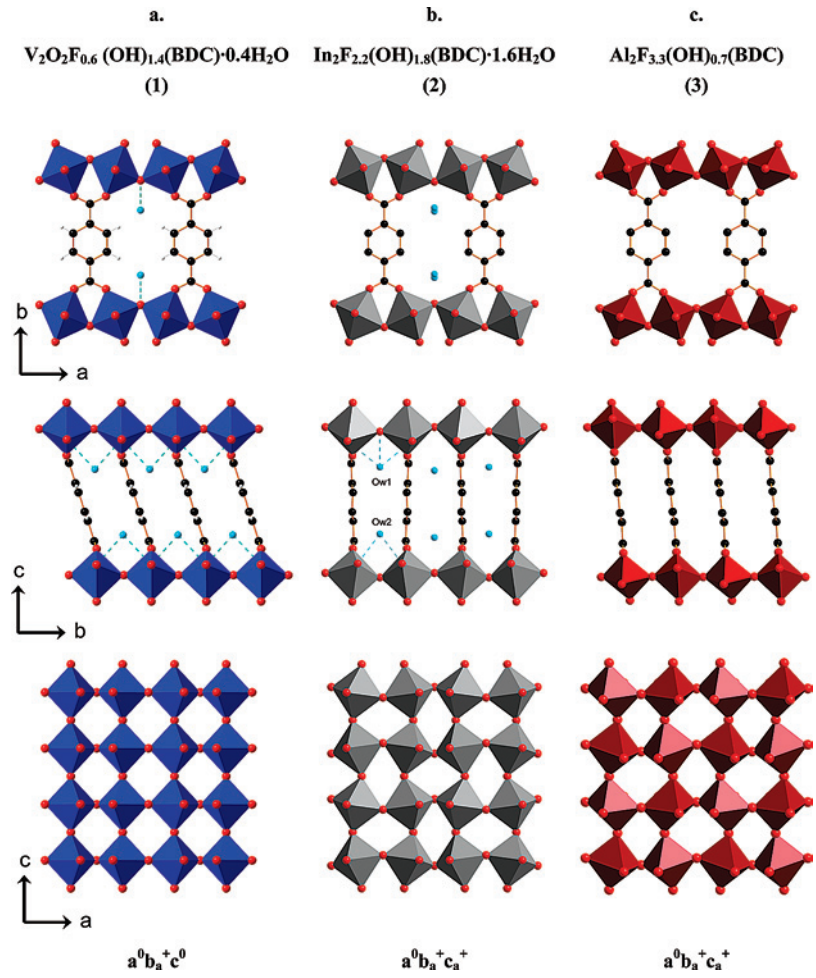

Figure 2. Structure of compounds **1**, **2**, and **3**. In compounds **1** and **2**, water molecules (light blue) are present between the layers and are hydrogen bonded to them. For monoclinic AlOHBDC, pseudo-orthorhombic projections are shown.

leading to the formation of a —O—V═O— chain along the *b* axis with bond lengths of 1.599(3) and 2.243(3) Å alternating along the chain. This alternation is actually less than that observed for V(V), for example, in V_2O_5 the two bonds range from 1.576(3) to 1.583(3) Å and from 2.800(3) to 2.805(3) Å.[35] The remaining V—O distances in **1** are 1.947(1) and 1.979(2) Å. The distorted octahedra are only tilted about *b*; at least one octahedral tilt is required in order for two adjacent metal centers to be bridged by two oxygen atoms from a single BDC carboxylate anion. The BDC carboxylate groups also impose an antiparallel arrangement of tilts in adjacent layers. An extension of Glazer's perovskite structure classification[36] has been developed for ABX_4 phases by Deblieck et al.[37] In this classification, the octahedral tilting is represented by the symbol $\mathbf{a}_u^i\mathbf{b}_v^j\mathbf{c}^k$ where *i*, *j*, *k* indicate the sense of the tilt about each of the principal axes (+, 0, −) and *u*, *v* indicate whether the tilt of octahedra in adjacent layers is parallel (p) or antiparallel (a). In this notation the structure of **1** is described by the symbol $\mathbf{a^0b_a^+c^0}$.

Adjacent layers in **1** are cross-linked by the BDC anions such that the —O—V═O— chains are oriented in the opposite sense in each pair of layers. The opposite orientation of the —O—V═O— chains results in a tilting of the BDC anions about the *a* axis relative to the layers. The interlayer space contains water molecules that are weakly hydrogen bonded to the equatorial oxygen atoms that are perpendicular to the —O—V═O— chain (the O---O separations are 2.816(8) and 2.865(8) Å, and the sites are only partially occupied presumably because of the increased hydrophobic nature of the interlayer. The water molecules are easily removed as seen from the thermogravimetric data (vide infra).

The structure of $In_2F_{2.2}(OH)_{1.8}(BDC)\cdot 1.6H_2O$ (**2**) (Figure 1b) is related to that of **1** but differs in several important structural and chemical features. The In^{3+} ion is coordinated to six L atoms (L = O and/or F) in distorted octahedral geometry. The four equatorial distances (In—OH, F bonds) are 2.106(4) Å and 2.136(6) Å while at the axial positions the In—OH,F bond lengths at 2.071(2) Å are now equal. The indium octahedra are linked through corner sharing hydroxyl and fluoride ions in the 001 and 100 directions to form a layer (Figure 1b) in which the octahedra are tilted about both *b* and *c* ($\mathbf{a^0b_a^+c_a^+}$). Two crystallographically distinct water molecules occupy the interlayer space and are hydrogen bonded to hydroxyl/fluoride ions within the layer; Ow1 has three long contacts at 3.112 (× 2) Å and 3.088 Å whereas Ow2 has two short contacts at 2.789 Å.

(35) Shklover, T.; Haibach, T.; Reid, F.; Nesper, R.; Novak, P. *J. Solid State Chem.* **1996**, *123*, 317–323.
(36) Glazer, A. M. *Acta Crystallogr.* **1972**, *B28*, 3384–3392.
(37) Deblieck, R.; Van Tenderloo, G.; Van Landuyt, J.; Amelinckx, S. *Acta Crystallogr.* **1985**, *B41*, 319–329.

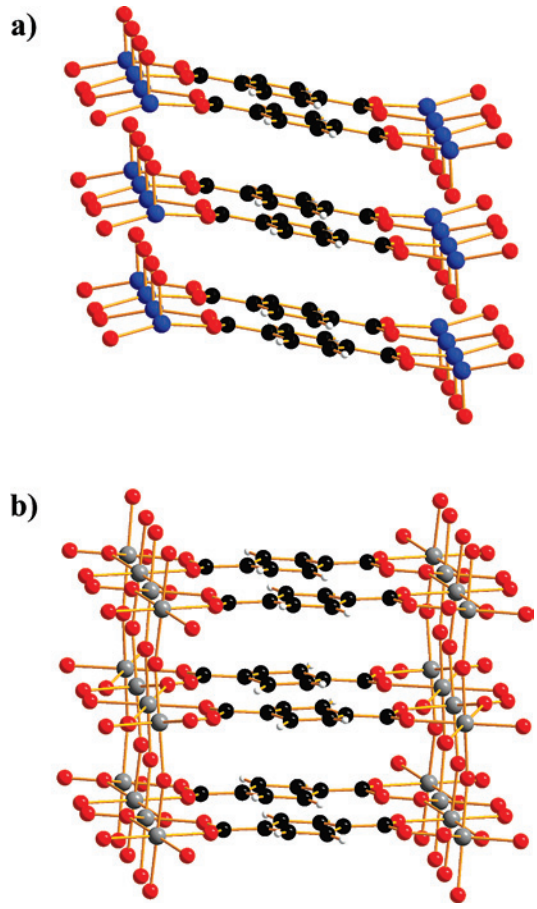

Figure 3. Idealized structures for compounds **1** (a) and **2** (b) where the OH and F groups have been replaced by oxygen.

$Al_2F_{3.3}(OH)_{0.7}(BDC)$ (**3**) (Figure 1c) also has a structure similar to that of compound **1** with noticeable differences. The symmetry is lowered from *Pnma* to $P2_1/m$. The AlL_6 (L = O and/or F) octahedra are distorted and are linked through corner sharing hydroxyl and fluoride ions in the 001 and 010 directions to form a layer (Figure 1c) in which the octahedral are tilted about b and c ($\mathbf{a^0b_a^+c_a^+}$). Adjacent layers are linked by the BDC ligands to form the 3D framework.

There are, therefore, two major structural differences between the geometrical features in **1** compared with those in **2** and **3**. Namely, the apical M−O bond distances alternate significantly in **1** along the *b* axis but they do not in **2** and **3**, and, second, the BDC ligands are tilted about the *a* axis in **1** but not in **2** or **3**. This is shown more clearly for the idealized structures of **1** and **2** in Figure 3 where of the OH and F groups have been replaced by O atoms. The bond alternation in **1**, just like in the perovskite family, is expected to create a substantial dipole moment along the *b* direction. However, as shown in Figure 3a, the dipole moments will alternate with respect to translation along the *c* axis and this, in turn, is established by the tilting of the BDC ligands about the *a* axis. The intriguing question is whether one might be able to design a material where the bond alternation is cumulative, in other words, a metal oxide where the BDC ligands are oriented in an fashion analogous to that in **2** (Figure 3b). We do not think that this is likely—the V−O bond alternation and the tilting of the BDC ligands are inextricably coupled. The bond alternation phenomenon is a consequence of transition metal d and p mixing with oxygen p which creates stronger M−O π bonds. This has been well-documented elsewhere.[38] Of course, this hybridization does not occur in **2** and **3**, and, therefore, the M−O distances along the *b* axis are equal. Furthermore, the vanadium atoms move up, out of the plane of the equatorial oxygen atoms. This also serves to re-enforce π bonding between V and O. This is shown on going from **4** to **5**.[39] In V_2O_5 the V atoms move 0.59 Å out of the plane of the equatorial O atoms. In compound **1** this distortion is 0.33 Å

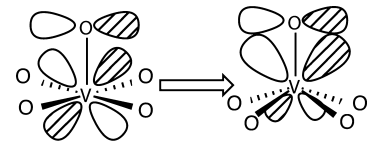

4 **5**

and in **2** it is 0.00 Å. It is in fact this movement that creates the tilting of the BDC ligands. Notice from **5** that when the V-carboxylate portion of the compound is planar, tilting is mandated for the BDC ligand. To estimate the energetic requirements for relaxing this stipulation, we carried out ab initio molecular orbital (MO) calculations using the hybrid density functional theory B3LYP on a model compound, $V_2O_3(OH)_4Bz^-$ where Bz = benzoate. The structure was optimized and some of the relevant bond lengths are indicated in **6** where the numbers in parenthesis are taken from the structure of **1**. The agreement between the model and observed structure is reasonable even though the model uses V(0).[40] A single point calculation was then carried out on structure **7** where the Bz ligand has been rotated to a horizontal position akin to that in **2**, and all other geometric variables were taken from **6**. Structure **6** was found to be 4.4 kcal/mol more stable than **7**.[41] This is a sizable energy difference. There are two electronic factors that contribute

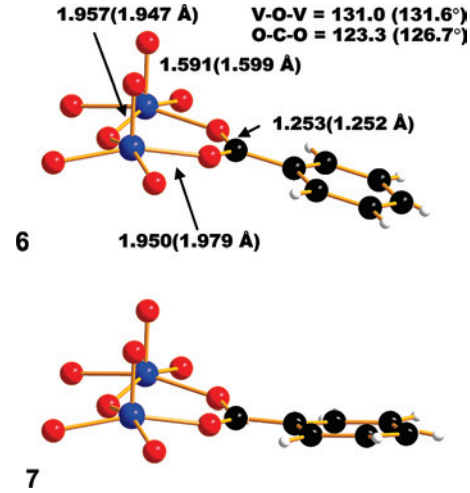

to the instability associated with **7**. First, as shown by going from structure **8** to **9**, the p atomic orbitals (AOs) on the two carboylate oxygens become hybridized in **9**. This in turn diminishes π delocalization within the carboxylate group. Second, overlap between the p AOs on the carboxylate

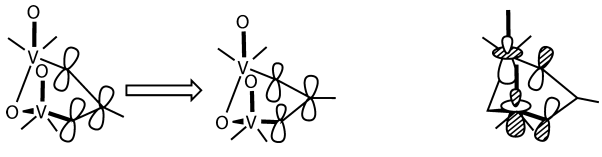

8 **9** **10**

oxygen atoms and the z^2 orbital on vanadium is maximized in **6**; see **10** for the antisymetric combination of z^2. The 4.4 kcal/mol energy difference on going from **6** to **7** is certainly large enough to prohibit the formation of a vanadium MOOF structure where the V−O bond alternations along the *b* axis are in phase and the BDC ligands lie parallel to the *ac* plane which would have the potential of creating a ferroelectric phase.

Thermogravimetric data for the compounds are given in the Supporting Information. Compound **1** (Supporting Information, Figure S1a) decomposes in two well separated steps. The first weight loss below 200 °C corresponds to the removal of the water molecules located between the layers of vanadium oxide. The second weight loss between 300 and 450 °C corresponds to the loss of 1 mol of framework BDC (38.48% measured, 39.83% calculated). TGA data for **2** (Supporting Information, Figure S1b) show that the decomposition now occurs in three steps. The first weight loss below 100 °C corresponds to the removal of the free water molecules between the layers. The second weight loss occurs in the temperature range of 300–400 °C. This corresponds to the removal of 0.9 H_2O from the framework (3.35% measured, 3.27% calculated). The third weight loss between 400 and 550 °C corresponds to the loss of 1 framework BDC (32.42% measured, 33.14% calculated). The TGA data for compound **3** (Supporting Information, Figure S1c) shows that it is anhydrous as synthesized and decomposes in a single step. The loss occurs in the temperature range of 550–700 °C and corresponds to the removal of 1 HF and 1 mol of framework BDC (61.77% measured, 63.02% calculated).

The infrared spectra of **1**, **2**, and **3** are also given in the Supporting Information, Figure S2). Characteristic stretching vibration bands of the OH group are found at approximately 3600 cm^{-1} for all three compounds. This is expected from the presence of the −OH group in all three structures. The lack of a band at approximately 1700 cm^{-1} characteristic of the free −C═O vibration, confirms the absence of free H_2BDC in compounds **1**, **2**, and **3**, as indicated earlier by the TGA analyses. Instead strong bands characteristic of O−C−O are observed at approximately 1400 cm^{-1}.

Conclusions

Three new MOOFs have been prepared, characterized, and their structural relationships investigated. The frameworks consist of inorganic layers constructed from corner sharing ML_6 octahedra (M = V, In, Al and L = OH, F) linked by BDC ligands. The layers show characteristic distortions that can be related to tilting of the ML_6 octahedra. In compound **1**, the distorted octahedra are only tilted about *b* ($\mathbf{a^0b_a{}^+c^0}$), bringing two apical oxygen atom positions close enough together to be bridged by a BDC anion. In compound **2** and **3**, the distorted octahedra are tilted about *b* and *c* ($\mathbf{a^0b_a{}^+c_a{}^+}$). The alternation of V−O bond distances along the *b* axis in **1** creates stronger V−O π bonding. This distortion creates a tilting of the BDC ligands about the *a* axis which in turn means that an antiferroelectric ordering is established. Model calculations show that it will be energetically costly to hold the BDC ligands parallel to the *ac* plane.

Acknowledgment. We thank the R. A. Welch Foundation and NSF DMR-0706072 for support of this work.

Supporting Information Available: X-ray crystallographic data, in CIF format, for the structure determinations of **1**, **2**, thermogravimetric analysis and infrared data for compounds **1**, **2**, and **3**, details of the powder diffraction determination of the structure of **3**, the full citation listing for reference 32, and a list of Cartesian coordinates for **6** and **7** along with energies (PDF). This material is available free of charge via the Internet at http://pubs.acs.org.

IC8000448

(38) Wheeler, R. A.; Whangbo, M.-H.; Hughbanks, T.; Hoffmann, R.; Burdett, J. K.; Albright, T. A. *J. Am. Chem. Soc.* **1986**, *108*, 2222–2236.

(39) Albright; T. A.; Burdett, J. K.; Whangbo, M.-H. *Orbital Interactions in Chemistry*; Wiley-Interscience: New York, 1985; p. 313–317.

(40) There are two complications when $V_2O_3(OH)_4Bz^{-2}$ is used where the oxidation state for vanadium is 4+. Firstly, the computational details will be sensitive to the spin state (singlet versus triplet). Secondly, several of the occupied MOs have positive eigenvalues even when using diffuse functions on oxygen and vanadium. This is not the case for $V_2O_3(OH)_4Bz^-$.

(41) Single point calculations on $V_2O_3(OH)_4Bz^{-2}$ using the structures for **6** and **7** resulted in an energy difference of 4.9 kcal/mol.